Supplementary Information

Giant light harvesting nano-antenna for single-molecule detection in ambient light

Kateryna Trofymchuk, Andreas Reisch, Pascal Didier, François Fras, Pierre Gilliot, Yves Mely, and Andrey S. Klymchenko

Supplementary Note 1. Theoretical calculation of FRET efficiency

Assuming a homogenous distribution of fluorophores, we can calculate the FRET efficiency inside NPs in case of absence of energy migration between donor dyes. To this end, we used the model of energy transfer to multiple acceptors in a homogeneous solution of donors and acceptors, without D–A diffusion. In the absence of homo-transfer among donors, the steady-state intensity of the donor is given by[1]

$$\frac{F_{DA}}{F_D} = 1 - \sqrt{\pi} * \gamma * \exp(\gamma^2)[1 - \mathrm{erf}(\gamma)].$$

In this expression $\gamma = \frac{A}{A_0}$, where A is the acceptor concentration. A_0 is the critical concentration representing the acceptor concentration that results in 76% energy transfer. It can be calculated by $A_0 = \frac{447}{R_0^3}$, where R_0 is the Förster radius expressed in Å. The error function erf(γ) is given by:

$$\mathrm{erf}(\gamma) = \frac{2}{\sqrt{\pi}} \int_0^{\gamma} \exp(-x^2)\, dx$$

The FRET efficiency could be calculated as:

$$E_{FRET} = 1 - \frac{F_{DA}}{F_D} = \sqrt{\pi} * \gamma * \exp(\gamma^2)[1 - \mathrm{erf}(\gamma)]$$

The Förster distance was calculated by: $R_0 = 0.211 \left[\frac{k^2 Q_D J(\lambda)}{n^4}\right]^{1/6}$.

The overlap integral $J(\lambda)$ was calculated using the FluorTools software.[2] Though R18 emission has a tendency to red shift and thus to induce an increased spectral overlap with an increase in its loading, the drop of its donor quantum yield leads to a decrease of the Förster distance (Table S6).

Supplementary Figures

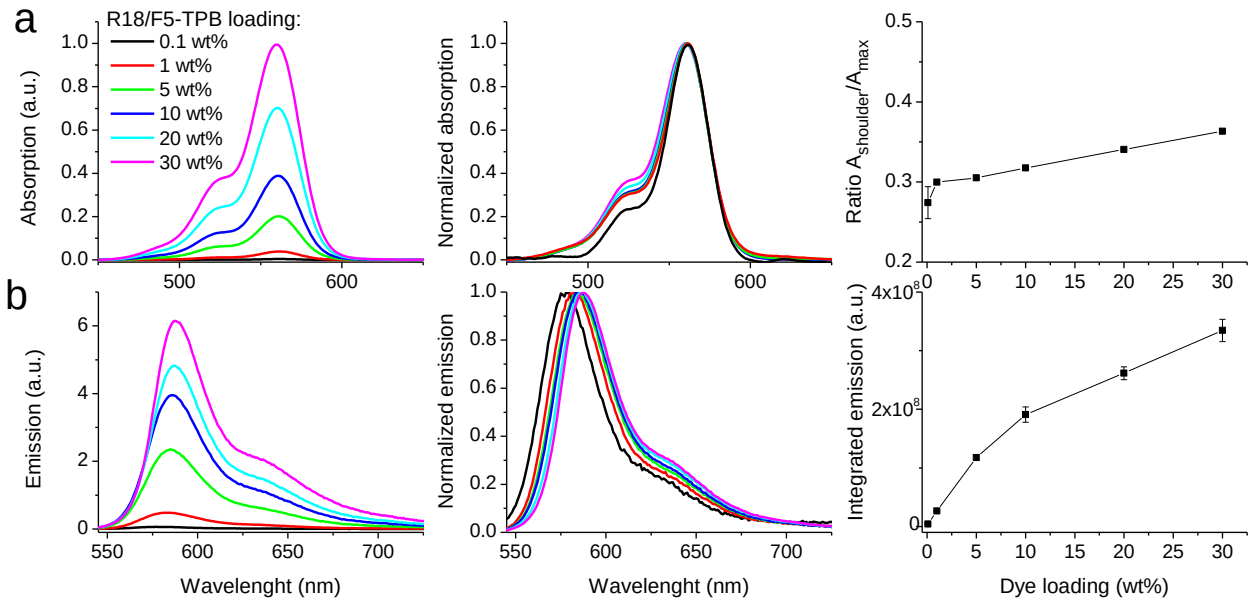

Supplementary Figure 1. Spectroscopic properties of PMMA-MA loaded with 0.1 wt%-30 wt% of R18/F5-TPB. (a) Absorption spectra (left), normalized absorption (middle) spectra and ratio of absorptions at wavelength of shoulder (λ = 525 nm) and maximum of absorption (right). (b) Emission spectra (left), normalized emission (middle) spectra and values of integrated emission intensity (right). Excitation wavelength was set at 530 nm. Error bars correspond to s.e.m. (n = 3).

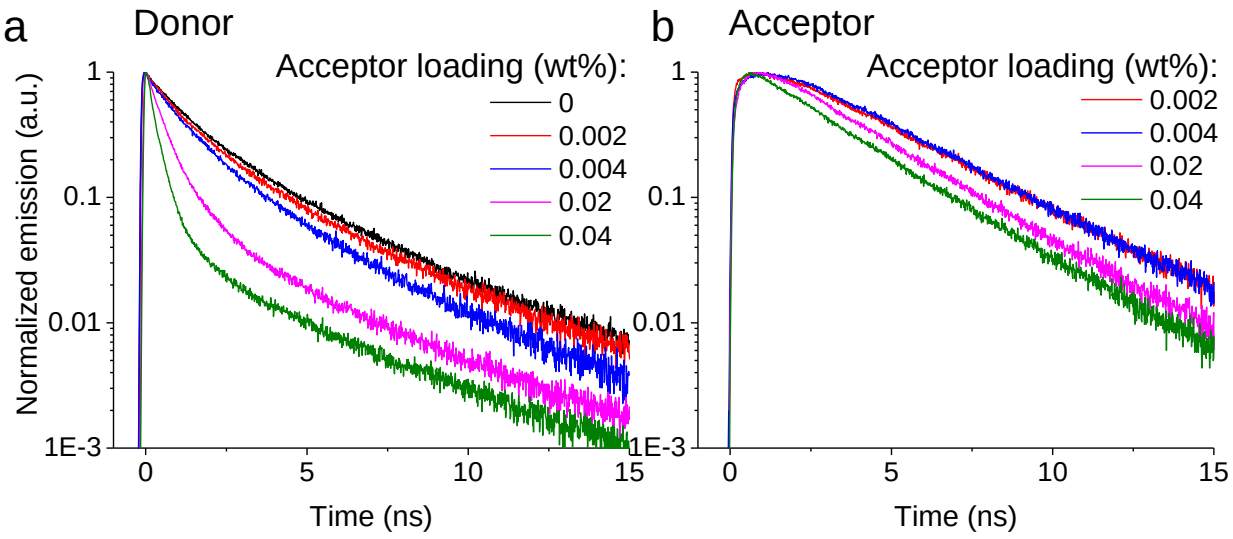

Supplementary Figure 2. Fluorescence emission decays of NPs loaded with 30 wt% of R18/F5-TPB and different amounts of acceptor detected at (a) donor emission wavelength (580 nm) and (b) acceptor emission wavelength (665 nm). Excitation wavelength was 480 nm.

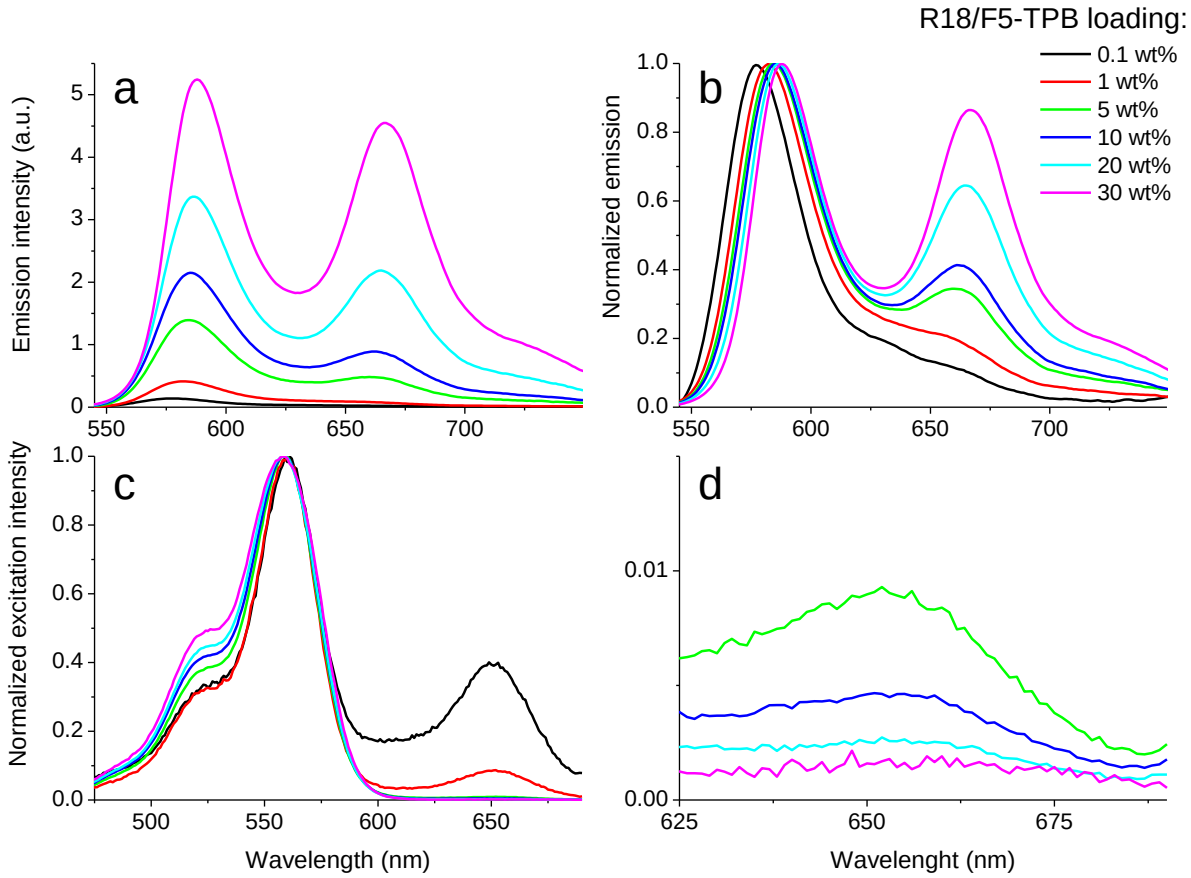

Supplementary Figure 3. Spectroscopic properties of FRET NPs loaded with different amounts of the donor dyes (R18/F5-TPB) while keeping the same level of acceptor dyes (0.004 wt %). (a) Emission spectra at 530 nm excitation wavelength. (b) Normalization on donor intensity emission spectra. (c) Excitation spectra describing the antenna effect. (d) Zoomed region of the excitation spectra focused on the excitation of the acceptor. Emission was detected at 700 nm.

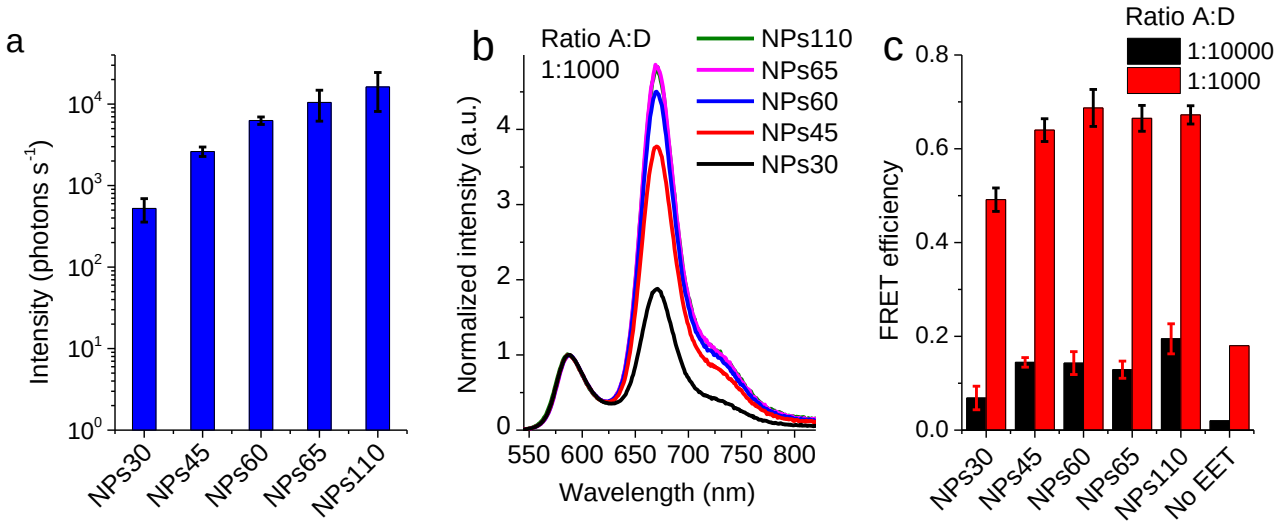

Supplementary Figure 4. Properties of nano-antennas as a function of NP size. (a) Single particle intensity of NPs loaded with 30 wt% of R18/F5-TPB immobilized on a glass surface under illumination of a 532 nm laser with power density of 0.1 W cm^{-2}. Error bars represent s.e.m. (n = 3). At least 500 particles were analysed in total per sample. (b) Fluorescence spectra of PMMA-MA FRET NPs of different size loaded with 30 wt% of R18/F5-TPB and DiD with Donor/Acceptor ratio 1,000:1. (c) FRET efficiency of NPs of different size loaded with 30 wt% of R18/F5-TPB and DiD. Donor/Acceptor ratios were 1,000:1 or 10,000:1. Error bars represent s.e.m. (n = 3).

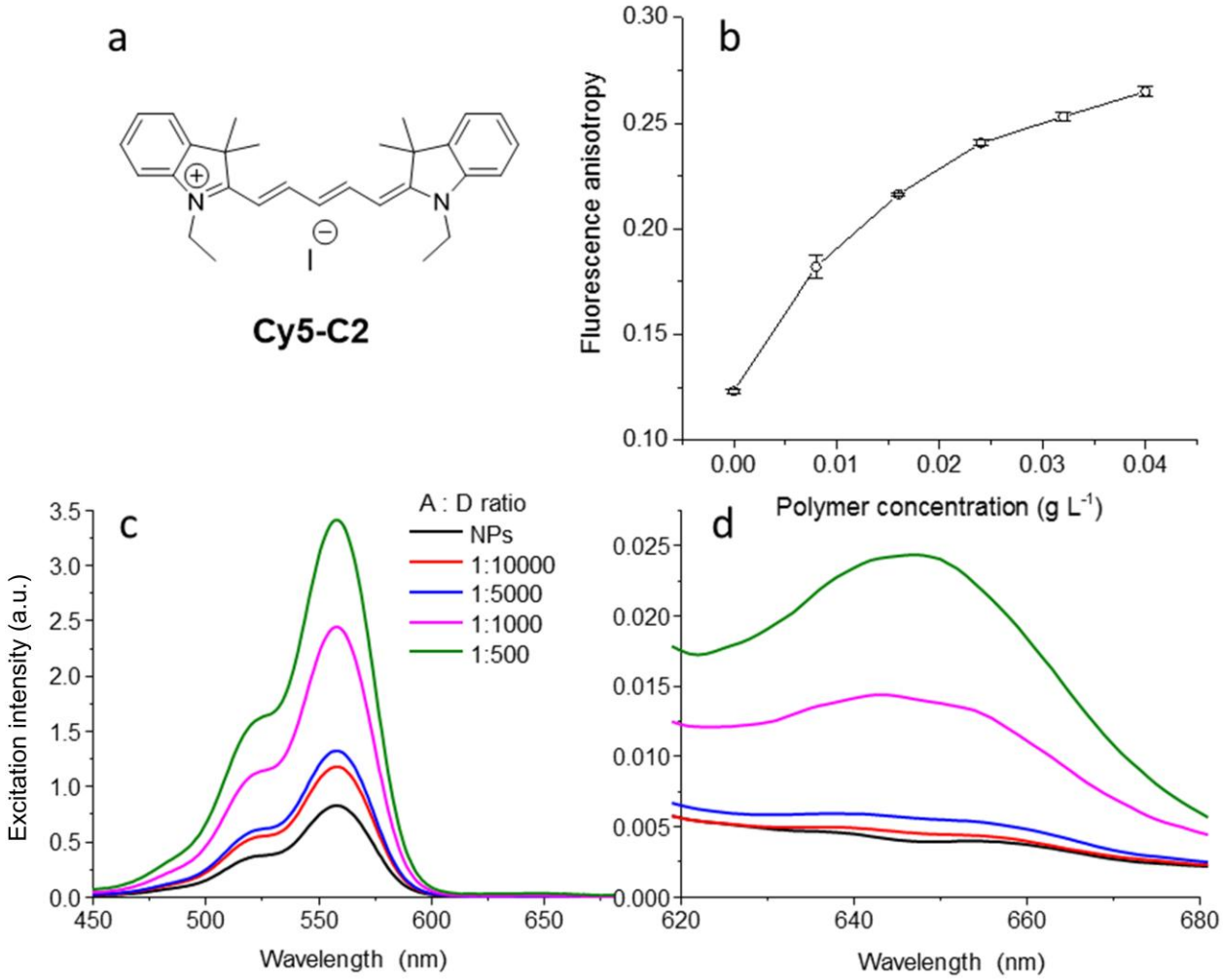

Supplementary Figure 5. Properties of FRET acceptor located on NPs surface. (a) Chemical structure of acceptor dye cyanine Cy5-C2. (b) Anisotropy value of Cy5C2 (15 nM) titrated with blank NPs of 40-nm size. Concentration of NPs is expressed in concentration of polymer (PMMA-MA). Acceptor concentration corresponds to 0.02 wt% with respect to maximal polymer concentration of NPs (0.04 g L^{-1}). Excitation wavelength was 620 nm. Emission wavelength was 655 nm. Error bars represent s.e.m. (n = 3). (c) Excitation spectra recorded at the acceptor emission (700 nm) of NPs 30 wt% R18/F5-TPB upon addition of Cy5-C2 describing the antenna effect. (d) Zoomed region of the excitation spectra focused on the excitation spectra of the acceptor.

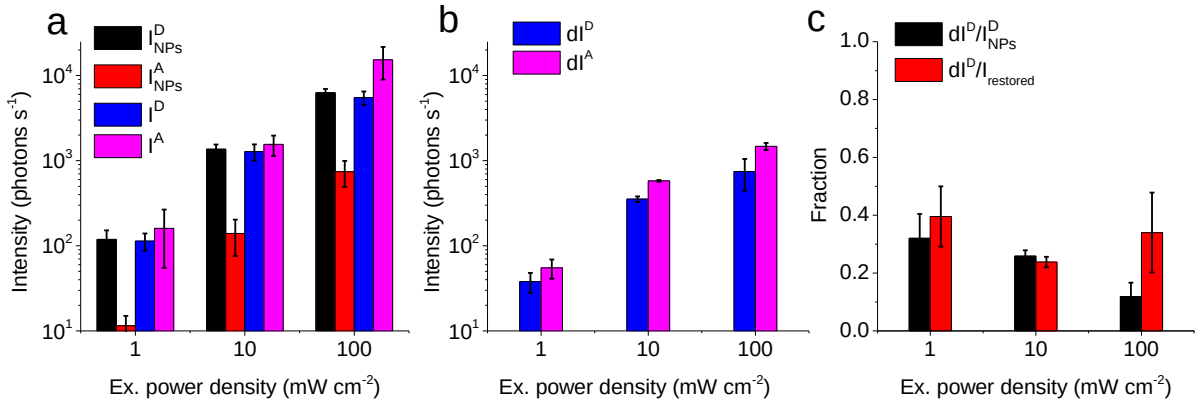

Supplementary Figure 6. Single particle intensities of nano-antennas and their stepwise changes. (a) Mean intensities of NPs60 without and with 0.004 wt% of acceptor detected at the donor and acceptor channels. I^D_{NPs} and I^A_{NPs} are intensities of NPs60 without acceptor at the donor and acceptor channels, respectively; I^D and I^A are intensities of NPs60 with 0.004 wt% acceptor at the donor and acceptor channels, respectively. Error bars represent s.e.m. (n ≥ 3). Total number of analysed particles was 200-500 per condition. (b) Gain in the donor intensity (dI^D) and drop in the acceptor intensity (dI^A) after acceptor photobleaching. (c) Ratio of gain in donor emission to intensity of NPs without acceptor (dI^D/I^D_{NPs}) and to intensity of the same FRET NP at the donor channel after acceptor photobleaching ($dI^D/I_{restored}$). For (b) and (c), the error bars represent s.e.m. (n ≥ 3). Total number of analysed particles was on average 50 per condition.

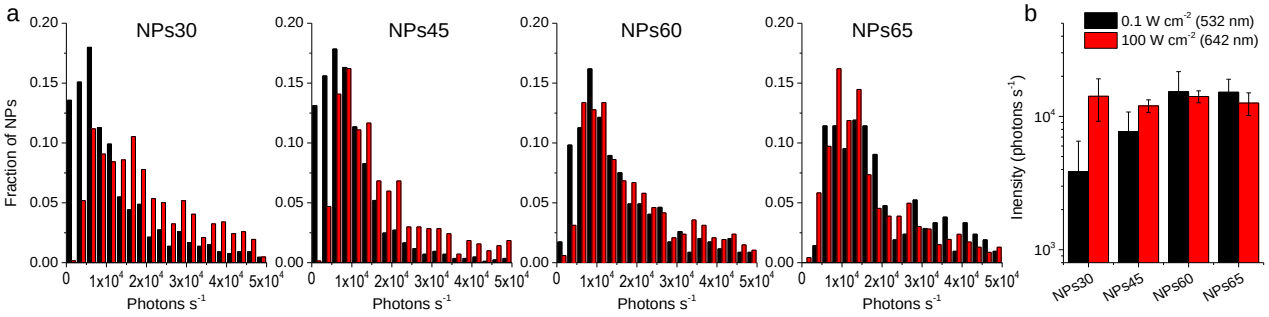

Supplementary Figure 7. Analysis of fluorescence intensities of acceptor in NPs of different sizes. (a) Intensities of single acceptors under excitation through FRET (532 nm with laser power density 0.1 W cm^{-2}) and direct excitation (642 nm with laser power density 100 W cm^{-2}). (b) Mean values based on log-normal fits of the intensity distribution for acceptors in NPs. Statistically, 1-2 acceptors are present inside NPs. The errors are s.e.m. (n = 3). At least 500 particles in total were analysed for each condition.

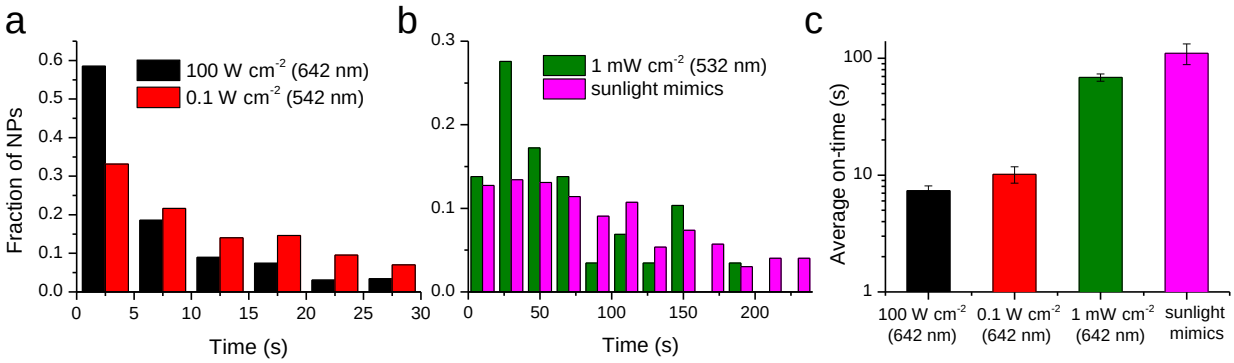

Supplementary Figure 8. On-time of acceptor dye inside NPs60 before photobleaching. (a) Histogram of on-time of acceptor before photobleaching under excitation at 642 nm with power density 100 W cm^{-2} and at 532 nm with power density 0.1 W cm^{-2}. (b) Under excitation at 532 nm with power density 1 mW cm^{-2} and excitation with source mimicking sunlight. (c) Average on-time of acceptor for a given excitation (error is s.e.m., n = 3). The total number of analysed particles was 100-300 per condition.

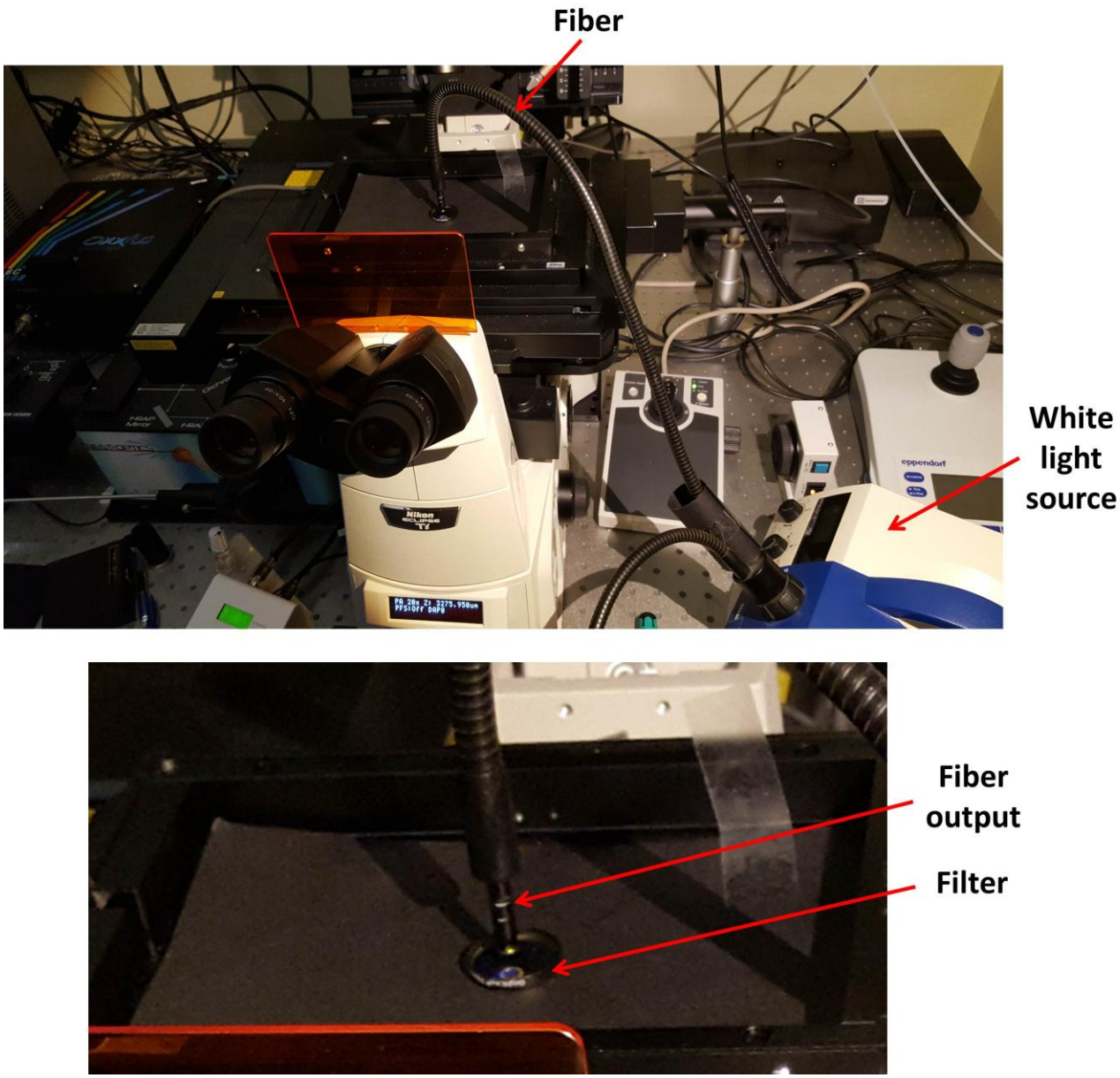

Supplementary Figure 9. Photo of the experimental setup that uses excitation by a divergent light, mimicking the sunlight. The divergent excitation light of the white light source was brought to the sample through a liquid optical fibre. The fibre output was pointed towards the sample (not visible in the figure) at ~2 cm distance. Filter (527 nm, 50 nm bandwidth) was placed between the fibre output and the sample. The light was collected from the bottom using 20X or 60X objective and recorded with a sCMOS camera.

Supplementary Tables

Supplementary Table 1. Hydrodynamic diameter and polydispersity of PMMA-MA NPs encapsulating different concentrations of R18/F5-TPB measured by DLS.[a]

NPs loading (wt%)	Diameter (nm)	PDI[b]
0	41	0.067
0.1	49	0.105
1	53	0.103
5	55	0.096
10	58	0.091
20	60	0.103
30[c]	67	0.101

[a] Statistics by volume was used in the analysis. The standard error of the mean (s.e.m.) on the hydrodynamic diameter from n = 3 measurements was ±2 nm for all NPs. [b] PDI is the polydispersity index. [c] According to TEM, the size of these NPs is (44 ±2) nm.

Supplementary Table 2. Time-resolved fluorescence parameters of PMMA-MA NPs loaded with different amounts of R18/F5-TPB, λ_{ex} = 480 nm and $\lambda_{detection}$ = 580 nm.[a]

R18/F5-TPB loading (wt%)	τ_{mean} (ns) [b]	τ_1 (ns)	α_1 (%)	τ_2(ns)	α_2(%)	τ_3(ns)	α_3(%)
0.1	4.20±0.03	4.20	100				
1	3.88±0.04	3.88	100				
5	3.29±0.19	3.29	100				
10	2.73±0.31	3.95	36	2.04	64		
20	2.54±0.09	4.05	40	1.54	60		
30	1.64±0.16	4.76	9	2.04	44	0.68	47

[a] The values of the individual lifetimes τ_i as well as their amplitudes α_i are reported. The mean lifetime is given by: $\tau_{mean} = \Sigma\, \tau_i\, \alpha_i /100$. [b] Error is s.e.m. (n = 3).

Supplementary Table 3. Dependence of Förster distance for homo FRET on dye loading.

NPs loading, wt%	Homo FRET distance R_0 (nm)	Average distance between encapsulated R18/F5-TPB dyes (nm)[a]
0.1	6.6	7.3
1	6.2	3.4
5	5.6	2.0
10	5.3	1.6
20	4.8	1.2
30	4.6	1.0

[a] Distance was calculated for isotropic distribution of fluorophores by: $l_{iso}=0.504/\sqrt[3]{c}$,[3] where c is the concentration of the dye.

Supplementary Table 4. Poisson distribution of the number of acceptors (0.004 wt %) encapsulated per NP of 44 nm diameter.[a]

Number of acceptor per NP	Fraction of NPs (%)
0	33
1	37
2	20
3	7
4	2
≥ 5	1

[a] The distribution corresponds to an average number of acceptors n = 1.2.

Supplementary Table 5. Time-resolved fluorescence parameters of PMMA-MA NPs loaded with 30 wt% of donor dyes and different amount of acceptor dyes, λ_{ex} = 480 nm and $\lambda_{detection}$ = 580 nm.[a]

Detection channel	Donor (580 nm)							Acceptor (665 nm)			
Acceptor loading (wt%)	τ_{mean} [b] (ns)	τ_1 (ns)	α_1 (%)	τ_2 (ns)	α_2 (%)	τ_3 (ns)	α_3 (%)	τ_1 (ns)	α_1 (%)	τ_2 (ns)	α_2 (%)
0.002	1.70±0.06	4.91	9	2.11	42	0.7	49	3.13	68	0.81	-32
0.004	1.60±0.05	5.21	9	2.05	39	0.68	53	3.24	62	0.80	-38
0.02	0.53±0.04	3.49	4	0.83	23	0.3	73	2.83	55	0.32	-45
0.04	0.35±0.01	3.64	2	0.63	14	0.22	84	2.64	47	0.19	-53

[a] The values of the individual lifetimes τ_i as well as their amplitudes α_i are reported. The mean lifetime is given by: $\tau_{mean} = \Sigma\, \tau_i\, \alpha_i /100$. [b] Error is s.e.m. (n = 3).

Supplementary Table 6. Estimation of FRET efficiency based on time-resolved data and the hypothetical number of donor dyes coupled to a single acceptor based on the data for NPs45.[a,b]

Acceptor loading (wt%)	Acceptor:Donor ratio	E_{FRET}^{local} (%)	$x_{\text{coupled donors}}$	$N_{\text{coupled donors}}$
0.002	1:10000	68 ± 11	0.21 ± 0.03	1250 ± 180
0.004	1:5000	67 ± 10	0.40 ± 0.06	2340 ± 360
0.02	1:1000	87 ± 12	0.71 ± 0.10	4180 ± 590
0.04	1:500	90 ± 12	0.86 ± 0.12	5080 ± 710

[a] E_{FRET}^{local} is the "local" FRET efficiency, which takes into account only the efficiency of dyes coupled by FRET to an acceptor inside NPs. It is estimated based on classical kinetics model:

$$E_{FRET}^{local} = \frac{k_{FRET}}{k_{FRET} + k_r + k_{nr}}$$

Where k_{FRET} is the rate constant of FRET, estimated from the raise time of the acceptor, $1/\tau_1$(acceptor), k_r and k_{nr} are the rate constants of radiative and non-radiative deactivation, respectively. E_{FRET}^{local} is different from FRET efficiency measured from the intensity of the donor dyes (E), because it takes into account all donor dyes inside NPs. The relation between E and E_{FRET}^{local} is the following:

$$E_{FRET}^{local} = x_{coupled\ donors} E$$

Where $x_{\text{coupled donors}}$ is the fraction of donor dyes inside NPs coupled to the acceptor with an efficiency E_{FRET}^{local}, assuming the simplified case of two populations of donor dyes: (i) not coupled to acceptor at all and (ii) undergoing FRET with E_{FRET}^{local} efficiency.

N (coupled donors) is the number of donor dyes coupled to a single acceptor ($x_{\text{coupled donors}} \times N_{dyes\ per\ NP}$).

[b] Error estimated based on s.e.m. of the rate constants.

Supplementary Table 7. Calculation of the theoretical FRET efficiency inside NPs with varied donor but constant acceptor (0.004 wt%) calculated in the absence of homo-FRET (EET) and comparison with the experimental FRET value.

NPs loading, (wt%)	$J(\lambda)$,[a] ($M^{-1}cm^{-1}nm^4$)	Q_D[b]	R_0[c] (Å)	Theoretical calculation [d] E_{FRET}	Experimental value E_{FRET}
0.1	9.73×10^{15}	0.99	70	6%	9%
1	1.13×10^{16}	0.86	69	6%	10%
5	1.29×10^{16}	0.76	70	6%	21%
10	1.33×10^{16}	0.58	67	5%	25%
20	1.38×10^{16}	0.4	63	4%	26%
30	1.41×10^{16}	0.3	61	4%	27%

[a] Overlap integral. [b] Quantum yield of donor dyes. [c] R_0 is the Förster distance for FRET pair R18 and DiD, which depends on the donor loading. [d] Theoretical FRET efficiency calculated in the absence of exciton diffusion.

Supplementary Table 8. Time-resolved fluorescence parameters of PMMA-MA NPs of different sizes loaded with 30 wt% of R18/F5-TPB, λ_{ex} = 480 nm and $\lambda_{detection}$ = 580 nm.[a]

Sample	τ_{mean} (ns)[b]	τ_1 (ns)	α_1 (%)	τ_2 (ns)	α_2 (%)	τ_3 (ns)	α_3 (%)
NPs30	1.88±0.17	5.98	9	2.64	36	0.68	55
NPs45	1.54±0.08	4.85	8	1.92	32	0.65	48
NPs60	1.69±0.06	4.43	8	2.00	52	0.77	40
NPs65	1.69±0.07	4.29	8	2.00	53	0.76	39
NPs110	1.68±0.11	3.99	9	2.02	50	0.79	41

[a] The values of the individual lifetimes τ_i as well as their amplitudes α_i are reported. The mean lifetime is given by: $\tau_{mean} = \Sigma\, \tau_i\, \alpha_i /100$. [b] Error is s.e.m. (n = 3).

Supplementary Table 9. Number of donor and acceptor molecules per NP, used for single particle studies.

Sample	Donor/NP[a]	Ratio A : D	Acceptor/NP[b]
NPs30	1,700	1:1,000	1.7
NPs45	5,900	1:5,000	1.2
NPs60	13,000	1:10,000	1.3
NPs65	17,000	1:20,000	0.85

[a] Estimation is based on NPs size measured by TEM. [b] Statistical value.

References

1 Lakowicz, J. R. *Principles of Fluorescence Spectroscopy*. (Springer, 2006).

2 *www.fluortools.com UV-Vis-IR Spectral Software 1.2*.

3 Colby, K. A. *et al.* Electronic energy migration on different time scales: concentration dependence of the time-resolved anisotropy and fluorescence quenching of lumogen red in poly (methyl methacrylate). *J. Phys. Chem. A* **114**, 3471-3482 (2010).